

Document downloaded from:

<http://hdl.handle.net/10251/108670>

This paper must be cited as:

Aurell, MJ.; González-Cardenete, MA.; Zaragoza, RJ. (2018). A new mechanism for internal nucleophilic substitution reactions. *Organic & Biomolecular Chemistry*. 16(7):1101-1112.  
doi:10.1039/c7ob02994b



The final publication is available at

<https://doi.org/10.1039/c7ob02994b>

Copyright The Royal Society of Chemistry

Additional Information

## New mechanism for internal nucleophilic substitution reactions.

 María J. Aurell,<sup>a</sup> Miguel A. González-Cardenete,<sup>b</sup> and Ramón J. Zaragoza<sup>\*a</sup>

 Received 00th January 20xx,  
Accepted 00th January 20xx

DOI: 10.1039/x0xx00000x

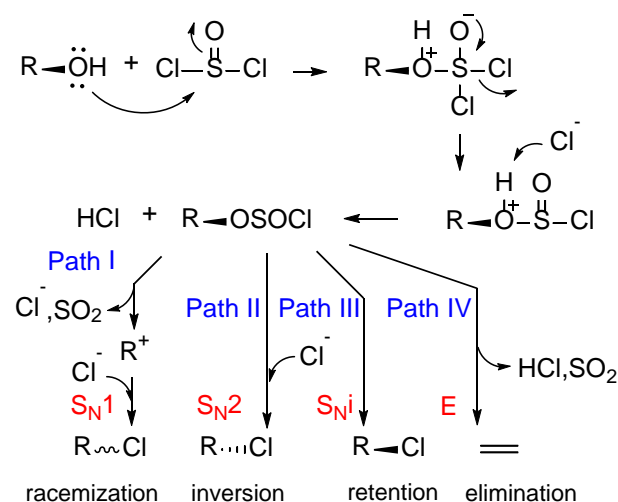
www.rsc.org/

A new mechanism of the classic internal nucleophilic substitution reactions  $S_{Ni}$  by means of computational studies in gas-phase, DCM and acetonitrile is reported. Despite the importance of the  $S_{Ni}$  mechanism, since the mid-1990s this mechanism has remained unexplored. The study has focused mainly on the comparison between the mechanisms postulated to date for the  $S_{Ni}$  reactions and a new mechanism suggested by us that fits better the experimental observations. The comparative study has been applied to the conversion of ethyl, neopentyl, isopropyl and tert-butyl chlorosulfites into the corresponding alkyl chlorides. This new mechanism occurs through two transition structures. For primary and secondary substrates, the first transition structure is a 6-center *syn*-rearrangement of the alkanesulfonyl chloride that produces the corresponding olefin by simultaneous expulsion of HCl and  $SO_2$ . The olefin, HCl and  $SO_2$  form a molecular complex. The final *syn* addition of HCl to the olefin leads to the alkyl chloride with retention of configuration. For tertiary substrates a variation of the previous mechanism is postulated with the intervention of *contact* ionic pairs. It is of great importance to emphasize that the new mechanism is able to explain some experimental observations such as the presence of olefins in this type of reactions and the low reactivity of some systems such as neopentyl chlorosulfite. Our results pave the way to a new mechanistic perspective in similar reactions which will need further studies and validation.

### 1-Introduction

A general method for converting alcohols to halides involves reactions with various halides of nonmetallic elements. Thionyl chloride, phosphorus trichloride, and phosphorus tribromide are the most common examples of this group of reagents.<sup>1-5</sup> Thionyl chloride is often preferable to other reagents due to its gaseous byproduct ( $SO_2$ ) for simplified purification.<sup>4</sup> The excess of thionyl chloride can also be readily removed by distillation or evaporation. Organic bases such as pyridine are often added to the reaction mixture because they provide a substantial concentration of chloride ion needed for the final reaction of the chlorosulfite intermediate. Recently, the use of catalysts such as titanium tetrachloride has been introduced for the stereoretentive chlorination of cyclic alcohols with thionyl chloride.<sup>6</sup> However, the reaction also proceeds in the absence of either bases or catalysts and under heating conditions.

The reaction of alcohols with thionyl chloride initially results in the formation of a chlorosulfite ester which is transformed subsequently into the chloride (Scheme 1).<sup>1-6</sup> In the first stage,



Scheme 1 Simplified mechanism for reaction of alcohol with  $SOCl_2$

the alcohol attacks  $SOCl_2$  and after expulsion of  $Cl^-$  and deprotonation, a chlorosulfite is formed. The mechanism for this stage is widely accepted and proceeds with retention of configuration at the carbon bearing the hydroxyl group.

The further course of the reaction will depend on both the structure of the chlorosulfite and the reaction conditions. The transformation of the chlorosulfite ester into a chloride, through a nucleophilic substitution, proceeds with racemization (Path I), inversion (Path II) or retention (Path III)

<sup>a</sup> Departamento de Química Orgánica, Universidad de Valencia, Dr. Moliner 50, 46100 Burjassot, Valencia, Spain.

<sup>b</sup> Instituto de Tecnología Química (UPV-CSIC), Universitat Politècnica de Valencia-Consejo Superior de Investigaciones Científicas, Avda. de los Naranjos s/n, 46022 Valencia, Spain.

E-mail: Ramon.J.Zaragoza@uv.es

† Electronic Supplementary Information (ESI) available. See DOI: 10.1039/x0xx00000x

of configuration at the carbon bearing the sulfite group (Scheme 1).<sup>1-12</sup> The decomposition of the chlorosulfite may also produce an alkene via an elimination mechanism (Path IV) (Scheme 1).<sup>4-7, 11</sup> Thus, several mechanisms might account for the variety of products formed under different reaction conditions.

For example, if racemization occurs, a  $S_N1$  mechanism is normally accepted.<sup>7</sup> In the cases of inversion of configuration, the suggested mechanism is of  $S_N2$  type<sup>7, 9, 11</sup> which may need the assistance of added base such as pyridine.<sup>7, 12</sup>

On the other hand, the retention of configuration is achieved mechanistically either through a double inversion in the presence of nucleophilic solvents<sup>9</sup> or via an internal nucleophilic substitution ( $S_{Ni}$ ).<sup>6, 7, 13</sup> The reaction of alcohols with thionyl chloride, with retention of configuration at the carbon bearing the hydroxyl group, is not the only case where a possible  $S_{Ni}$  mechanism is postulated. For example, the reactions of certain secondary alcohols with phosgene,  $PCl_5$  in liquid  $SO_2$ , or dry  $HBr$  to give halides, whose configurations are the same as those of the starting alcohols, have been classified as examples of the  $S_{Ni}$  reaction.<sup>7</sup>

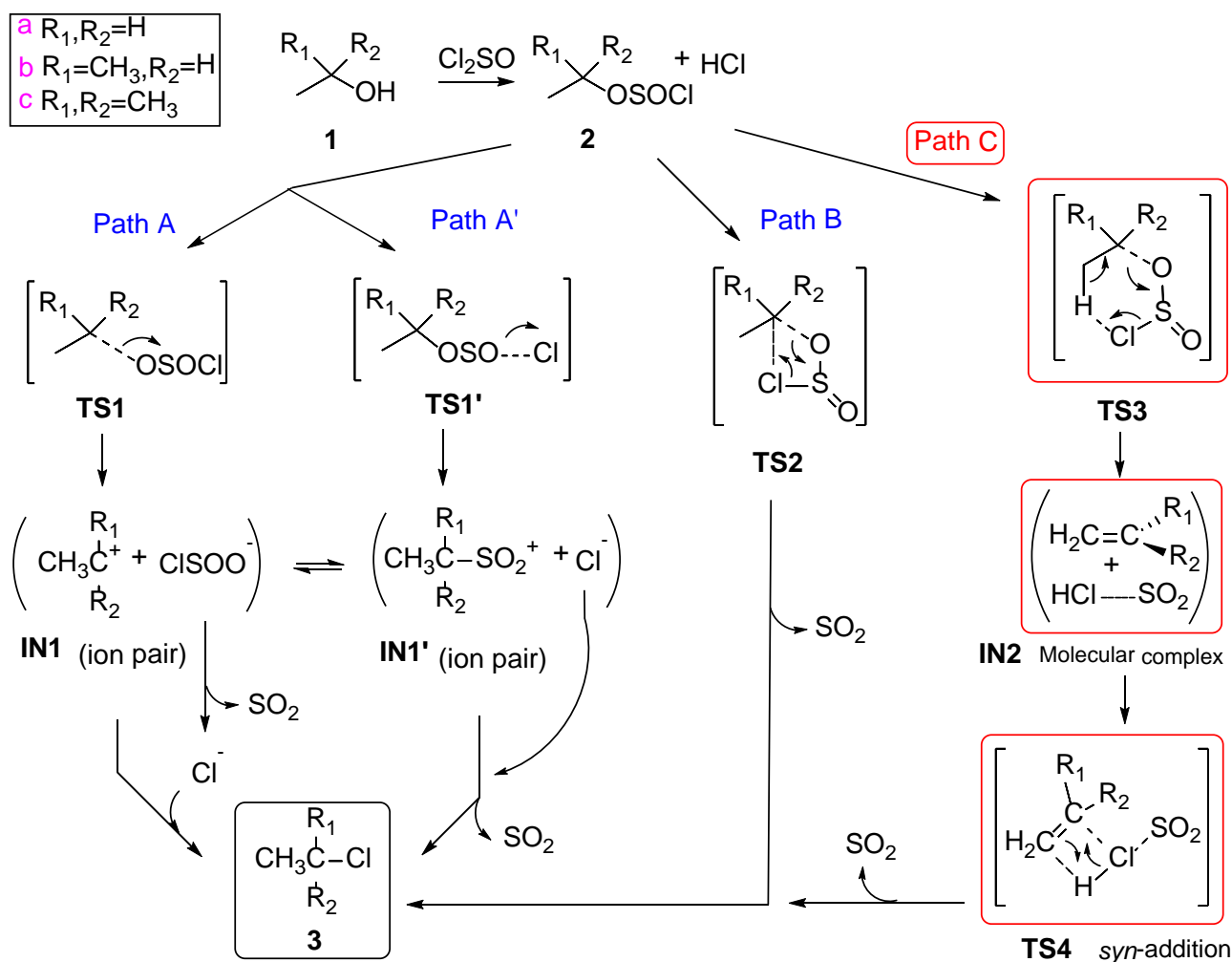
A recent work of synthesis<sup>14</sup> allowed us to perform a review on

this mechanism which indeed has not received much attention. For example, the  $S_{Ni}$  mechanism is not explicitly considered in some well-known textbooks. It is also ironic that chlorination with  $SOCl_2$  is a technique that is covered in most undergraduate organic chemistry textbooks, and is even performed in some undergraduate teaching laboratories, without mentioning the  $S_{Ni}$  designation.

The present paper reports the results of a detailed study, by means of computational studies, of the main mechanistic options suggested to date for the  $S_{Ni}$  reaction (Scheme 2, paths A/A' and B), comparing them with a new postulated mechanism (Scheme 2, path C). The study has been applied to the conversion of a chlorosulfite ester into an alkyl chloride. The new mechanism is able to explain some experimental observations such as the presence of olefins in this type of reactions and the low reactivity of some systems such as neopentyl chlorosulfite.

## 2-Results and Discussion

In Scheme 2, the three studied routes for the conversion of alcohol **1** into the corresponding alkyl chloride **3**, through



**Scheme 2** Transformation of an alcohol to the corresponding chloroalkane via a  $S_{Ni}$  mechanism.

chlorosulfite ester **2**, by a  $S_{Ni}$  mechanism with retention of configuration at the carbon bearing the hydroxyl group, are shown. Path A/A' and B describe current accepted reaction mechanisms. Path C is a new alternative suggested by us. Here, our work demonstrates that path C is a superior energetically favorable reaction path.

In path A/A', the chlorosulfite ester is converted into the ion pair **IN1/IN1'**. This **IN1/IN1'** undergoes front-side attack of the  $Cl^-$  and loss of  $SO_2$  to give the alkyl chloride **3** with retention of configuration. Lewis and Boozer<sup>1,8</sup> proposed a multistep ionization mechanism, with the ion-pairs **IN1** and **IN1'**, to explain the formation of alkyl chloride **3**. Cram<sup>7</sup> also suggested that the  $S_{Ni}$  mechanism involves ion-pair intermediates and that the  $S_{Ni}$  reaction differs from the  $S_{N1}$  reaction only in the sense that the departing group is complex, and that the anion of the first ion-pair can decompose internally faster than an anion can react at the rear of the carbon undergoing substitution.

Subsequently King et al.<sup>15</sup> proposed that the hydrolysis of *tert*-butyl chlorosulfite (**2c** in Scheme 2), in water or methanol-chloroform mixture, is an ionization to the *tert*-butyl cation and the chlorosulfite anion (path A in Scheme 2) followed by further reaction of these species. Moreover, Schreiner, Schleyer and Hill<sup>16, 17</sup> concluded that the ionization of alkanesulfonyl chlorides in polar solvents, e.g., acetonitrile, yields  $ROSO^+ + Cl^-$  for R = primary alkyl group, and  $R^+ + OSOCl^-$  for R = secondary or tertiary alkyl group. The formation of ion-pairs always involves the competition between the  $S_{Ni}$  (front-side attack),  $S_{N2}$  (back-side attack) and  $S_{N1}$  (front- and back-side attack) mechanisms.

On the other hand, path B (Scheme 2) corresponds to the direct conversion of alkanesulfonyl chloride **2** into the alkyl chloride **3** through a unique transition structure **TS2**. This transformation was depicted as proceeding via a 4-center rearrangement of the alkanesulfonyl chloride.<sup>7, 16, 17</sup> This option permits a pure  $S_{Ni}$  mechanism by producing only the front-side attack with retention of configuration.

It is interesting to note that frequently, significant amounts of olefin are formed during decomposition of alkanesulfonyl chlorides.<sup>7, 16</sup>

Finally, path C (Scheme 2) represents our proposed  $S_{Ni}$  mechanism, which illustrates how olefins are formed and why neopentyl chlorosulfite displays such low reactivity. In this case, the conversion of the alkanesulfonyl chloride **2** into the alkyl chloride **3** occurs through two transition structures **TS3** and **TS4**. The transition structure **TS3** is a 6-center *syn*-rearrangement of the alkanesulfonyl chloride that produces the corresponding olefin by simultaneous expulsion of the HCl and  $SO_2$ . This mechanism is similar to the pyrolytic eliminations of esters (Ei mechanism) to give olefins.<sup>18</sup> The olefin, the HCl and the  $SO_2$  form a molecular complex (**IN2**). The *syn* addition of HCl to the olefin through the transition structure **TS4** leads to the alkyl chloride **3** with retention of configuration.

With the aim of comparing the three alternative routes in Scheme 2 (paths A-C), we have carried out computational

studies using ethyl chlorosulfite (**2a**) as a primary substrate, isopropyl chlorosulfite (**2b**) as a secondary substrate, and *tert*-butyl chlorosulfite (**2c**) as a tertiary substrate. To facilitate reading this article, we use the letters **a**, **b** and **c** when referring to primary substrate, secondary substrate and tertiary substrate, respectively.

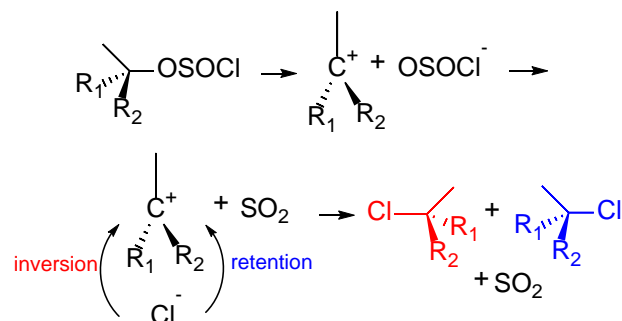
Firstly, we make a brief description of the calculations previously made in similar systems and then, for each of the substrates, the calculations made by us. To this end, the energy and geometry discussion is made initially on the basis of data in gas-phase, and subsequently the effect of solvent is introduced. To study this effect, the calculations have been carried out in a solvent of high polarity such as acetonitrile ( $CH_3CN$ ) and in a solvent of medium polarity such as dichloromethane (DCM) (see 2.2 Computational methods).

### 2.1 Previous calculations.

Schreiner, Schleyer and Hill,<sup>16</sup> using semiempirical and ab initio calculations, concluded that primary alkanesulfonyl chlorides in polar solvents, e.g.,  $CH_3CN$  should ionize to give preferentially an alkyl sulfinyl cation ( $ROSO^+$ ) and  $Cl^-$  (path A' in Scheme 2). The formation of the ion pair  $ROSO^+Cl^-$  precedes the loss of  $SO_2$  and is a key step in the  $S_{Ni}$  reaction. This mechanism has been named by the authors as  $S_{N2i}$ . They exclude the possible ionization to give the carbocation  $R^+$  and the anion  $SO_2Cl^-$  (path A in Scheme 2). Their conclusions are based on the relative energies calculated for the ions  $ROSO^+$  and  $Cl^-$  versus the ions  $R^+$  and  $SO_2Cl^-$ .

Subsequently, the same authors<sup>17</sup> examined the transition structures for the front-side ( $S_{Ni}$ ) and back-side ( $S_{N2}$ ) substitutions of methyl and ethyl chlorosulfite in gas-phase and in solution. They conclude that for primary alkyl chlorosulfites, such as ethyl chlorosulfite, the front-side attack, through a transition structure like **TS2** (see Scheme 2), is always preferred in the gas-phase and in solution.

These authors also concluded that secondary and tertiary alkanesulfonyl chlorides should ionize to give the carbocation  $R^+$  and the chlorosulfinyl anion  $SO_2Cl^-$  (path A in Scheme 2).<sup>16,17</sup> Subsequently, the anion  $SO_2Cl^-$  is fragmented into  $SO_2$  and  $Cl^-$  (Scheme 3). The chloride ion, can front-side attack to the  $R^+$  leading to retention of configuration (named by the authors as  $S_{N1i}$ ) or back-side attack leading to inversion of configuration.



Scheme 3 Ionization of secondary and tertiary alkanesulfonyl chlorides.

## 2.2 Computational methods

All calculations were carried out with the Gaussian 09 suite of programs.<sup>19</sup> Initially, density functional theory<sup>20</sup> calculations (DFT) have carried out using the B3LYP<sup>21</sup> exchange-correlation functionals, together with the standard 6-31G\*\* basis set, in gas phase.<sup>22</sup> The stationary points were characterized by frequency computations in order to verify that TSs have one and only one imaginary frequency. Subsequently, since the mechanism involves ionic species the inclusion of solvent effects have been considered by using a relatively simple self-consistent reaction field (SCRF) method<sup>23</sup> based on the polarizable continuum model (PCM) of Tomasi's group.<sup>24</sup> Geometries have been fully optimized with PCM. As solvents we have used DCM and acetonitrile. The intrinsic reaction coordinate (IRC) paths<sup>25</sup> were traced in order to check the energy profiles connecting each TS to the two associated minima of the proposed mechanisms using the second order González-Schlegel integration method.<sup>26</sup> In the case of problematic IRCs (flat PES in the vicinity of TS), a relaxed scan was performed.

Due to the presence of ionic pairs (in **2b** and **2c**) we performed a more precise study by the introduction of four explicit solvent molecules of acetonitrile.

The values of enthalpies, entropies and free energies in vacuum (gas phase), DCM and acetonitrile were calculated with the standard statistical thermodynamics at 298.15K and 1 atm (in gas phase) and 1 M (in solvent).<sup>22</sup>

The electronic structures of stationary points were analyzed by the natural bond orbital (NBO) method.<sup>27</sup> Finally, stationary points involved in these reactions were optimized, in DCM and acetonitrile, using the MPWB1K hybrid meta functional<sup>28</sup> together with the 6-31++G\*\* basis set.<sup>22</sup> This level of theory has shown to have good results for combinations of thermochemistry and thermochemical kinetics in processes including weak interactions.<sup>28</sup> Also single point at B3LYP-D3/def2TZVP level and M062X/cc-pVTZ level over MPWB1K geometries (B3LYP-D3/def2TZVP//MPWB1K/6-31++G\*\* and M062X/cc-pVTZ//MPWB1K/6-31++G\*\*) were performed in acetonitrile. Enthalpies, entropies and free energies were calculated using the values of the standard statistical thermodynamics obtained previously at B3LYP/6-31G\*\* level.

### 2.3 Conversion of ethyl chlorosulfite (**2a**) into chloroethane (**3a**)

The relative energies ( $\Delta G$ ) in gas-phase, DCM and  $\text{CH}_3\text{CN}$  associated with the conversion of **2a** into **3a** are given in Fig. 1 (see also Table S1 and Fig. S1a-1/S3a-3 of the ESI). Fig. 2 shows the geometries of the more relevant species.

#### 2.3.1 In gas-phase.

Only was possible to locate the transition structure **TS2a** corresponding to the path B (Scheme 2), and the transition structures **TS3a** and **TS4a**, and intermediate **IN2a** corresponding to the path C suggested by us. The transition structure **TS2a** corresponding to the path B is a 4-center *syn*-rearrangement (Fig. 2). The **TS3a** is a 6-center *syn*-rearrangement, similar to the *Ei* pyrolytic eliminations of esters,<sup>18</sup> and leads to the corresponding olefin by simultaneous expulsion of HCl and  $\text{SO}_2$ . The olefin, HCl and  $\text{SO}_2$

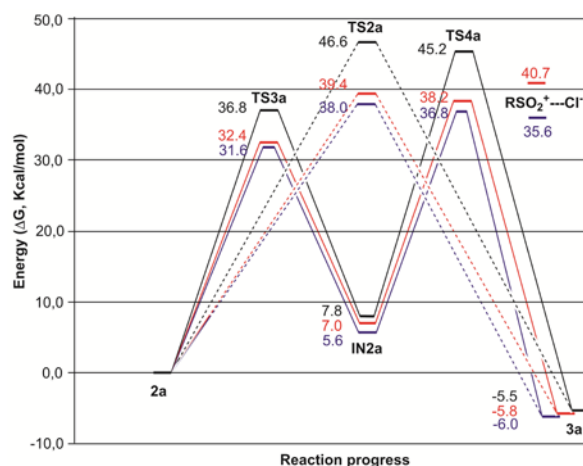


Fig. 1 Free energy profile ( $\Delta G$  in  $\text{kcal mol}^{-1}$ ) for the conversion of **2a** into **3a** in vacuo (in black), DCM (in red) and  $\text{CH}_3\text{CN}$  (in blue). The striped and solid lines correspond to the path B and path C (Scheme 2), respectively.

form a molecular complex **IN2a** quite stable. The regio- and stereoselective addition of HCl to the olefin through the transition structure **TS4a** finally leads to chloroethane **3a**. It should be noted that a carbocation is never formed, as it is postulated in the normal mechanism of HCl addition to olefins. The Gibbs free energy of the transition structure **TS4a** is  $45.2 \text{ kcal mol}^{-1}$  higher than that of **2a** (but  $1.4 \text{ kcal mol}^{-1}$  lower to  $\Delta G$  of **TS2a**), being in this case the rate limiting step for the conversion of **2a** into **3a**. Therefore, in terms of energy in gas-phase, the path C (Scheme 2) is more favorable than the path B (Scheme 2) (see 2.3.1-extended of the ESI for more details).

#### 2.3.2 Solvent effects in geometries, charges and energies.

We have selected two different solvent parameters (DCM and  $\text{CH}_3\text{CN}$ ) to cover the solvent polarities. In the calculations in DCM and acetonitrile for the ions  $\text{CH}_3\text{CH}_2\text{OSO}^+ + \text{Cl}^-$ ,  $\text{CH}_3\text{CH}_2^+ + \text{SO}_2\text{Cl}^-$  (Table S1), a preference for ionization through path A' in Scheme 2 ( $\text{CH}_3\text{CH}_2\text{OSO}^+ + \text{Cl}^-$ ) was observed. However, it was not possible to locate neither the ion pair  $\text{CH}_3\text{CH}_2\text{OSO}^+\text{Cl}^-$  (**IN1'a**) nor the corresponding transition structure **TS1'a** in either DCM or  $\text{CH}_3\text{CN}$ . For example, on using **2a** and setting the

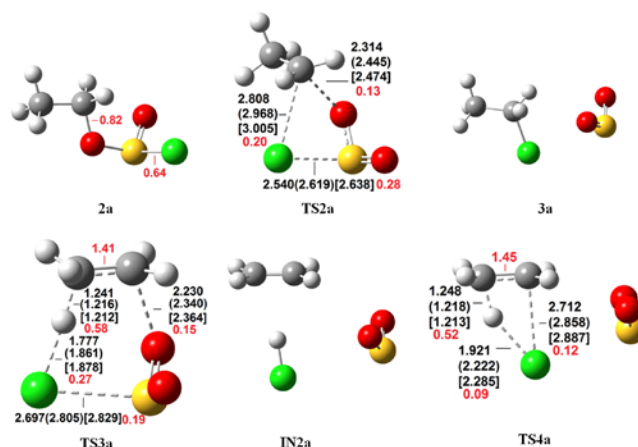


Fig. 2 Geometries, in gas-phase, of the species involved in the conversion of ethyl chlorosulfite **2a** into chloroethane **3a**. The bond lengths (in black) are given in angstroms. Values in parentheses and in brackets correspond to the bond lengths in DCM and  $\text{CH}_3\text{CN}$ , respectively. The bond order (BO), in DCM, is in red.

distance Cl-SO<sub>2</sub>CH<sub>2</sub>CH<sub>3</sub> in steps of 0.2 Å, the energy profile in CH<sub>3</sub>CN rises to a maximum (distance Cl-S ≈ 6 Å), and then stabilizes (see Fig. S5a of the ESI). When the bond Cl-S was freed, the calculations converged to give the starting chlorosulfite **2a** without passing through any transition structure. In order to obtain approximate calculations, the distance RSO<sub>2</sub><sup>+</sup>---Cl<sup>-</sup> was set at 6 Å. In this situation, the ΔG values obtained for the molecular complex CH<sub>3</sub>CH<sub>2</sub>OSO<sup>+</sup>---Cl<sup>-</sup> are 40.7 and 35.6 kcal mol<sup>-1</sup> in DCM and acetonitrile, respectively, above the energy value of ethyl chlorosulfite **2a**. The ΔG values obtained for the molecular complex CH<sub>3</sub>CH<sub>2</sub>OSO<sup>+</sup>---Cl<sup>-</sup> is similar to the values obtained for the transition structures **TS2a**, **TS3a** and **TS4a** (see Fig. 1), what makes possible the presence of these ions in polar solvents such as CH<sub>3</sub>CN.

With regard to the transition structures **TS2a**, **TS3a** and **TS4a**, the inclusion of the solvent does not produce significant geometric changes. On increasing the polarity (gas-phase < DCM < CH<sub>3</sub>CN), it is observed a light increase in the length of the bonds either being formed or broken except the bonds H-C(2) (**TS3a** and **TS4a**) in which the increase in polarity produces a shorter bond (Fig. 2).

The extent of bond formation along a reaction pathway is provided by the concept of bond order (BO). The BO values, in DCM, of some bonds are summarized in Fig. 2. In **TS2a** the BO values of 0.13, 0.28 and 0.20 for the C(1)-OSO, Cl-SO<sub>2</sub> and C(1)-Cl bonds, respectively, indicate that formation of these bonds is delayed. In the transition structure **TS3a** the C(1)-OSO, Cl-SO<sub>2</sub> and Cl-H bonds are also delayed (BO values of 0.15, 0.19 and 0.27, respectively), while the bond H-C(2) is quite advanced (BO value of 0.58). Finally, at **TS4a**, the BO values of 0.12 (C(1)-Cl), 0.09 (Cl-H) and 0.52 (C(2)-H) confirm (see 2.3.1-extended of the ESI) the initial transference of the H atom of HCl to the olefinic C(2) before the formation of the bond C(1)-Cl.

The natural charges are a valuable tool for the prediction of the ionic character of the involved species in a reaction mechanism. In this case, they helped us to establish the carbocationic character of the hydrocarbon fragments of the different species, and its variation changing the polarity of the solvent. All the obtained transition structures (**TS2a**, **TS3a** and **TS4a**) possess an important carbocationic character, which increases with the increase in polarity (Table S8 of the ESI). The transition structure **TS3a** possesses the least carbocationic character in any medium, while **TS4a** has the highest carbocationic character.

The inclusion of the solvent produces a strong stabilization of all species (between 3.8 and 11.0 kcal mol<sup>-1</sup> in DCM and between 4.4 and 13.0 kcal mol<sup>-1</sup> in CH<sub>3</sub>CN), being this stabilization smaller in **2a** and **3a** with lesser ionic character (between 3.8 and 4.8 kcal mol<sup>-1</sup>) and higher in **TS3a** (between 8.1 and 9.6 kcal mol<sup>-1</sup>) and **TS2a/TS4a** (between 10.7 and 13.0 kcal mol<sup>-1</sup>) (see Table S1 of the ESI), in agreement with their higher cationic character. The result is that in the studied solvents (DCM or CH<sub>3</sub>CN) the free energy barrier (see Fig. 1) for the conversion of **2a** into **3a** is lower than in gas-phase, regardless of the mechanism. In addition, when passing from

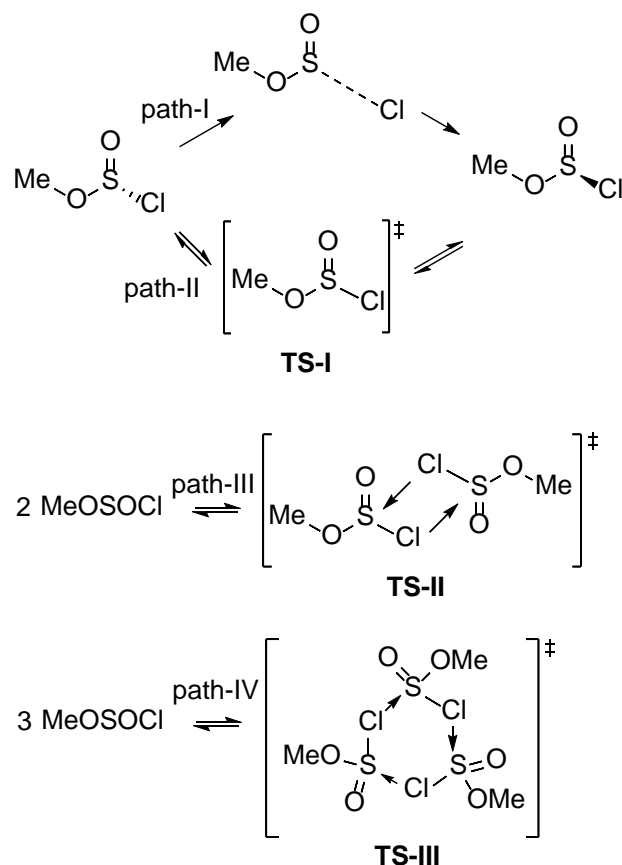
the gas-phase to solvents of increasing polarity, a flattening around the transition structures in the corresponding IRCs is observed (compare Fig. S1a-1/S1a-3, S2a-1/S2a-3 and S3a-1/S3a-3 of the ESI).

With independence of the medium, the transition structure **TS4a** is about 1.2-1.4 kcal mol<sup>-1</sup> more stable than the transition structure **TS2a**. Based on these results we can suggest that for a primary substrate the preferred mechanism, for the conversion of an alkyl chlorosulfite into the corresponding chloride with retention of configuration, would be through the two steps (**TS3a** and **TS4a**) of path C in comparison with the path B in one step (**TS2a**).

It should be noted that in the case of ionization of a primary alkyl chlorosulfite (for example in acetonitrile) to give the RSO<sub>2</sub><sup>+</sup> and Cl<sup>-</sup> ions, the Cl<sup>-</sup> ion must subsequently produce the substitution of the SO<sub>2</sub>. In order to maintain the retention of configuration, the Cl<sup>-</sup> ion attack would imply a transition structure similar to **TS2a** or **TS3a** (followed by **TS4a**), and therefore these TSs would control the course of the reaction.

It is of great importance to emphasize that none of the previously postulated mechanisms (A' or B) can explain the low rate constant for the decomposition of neopentyl chlorosulfite.<sup>16</sup> However, it can be explained by the absence, in this case, of the new postulated C mechanism. For the mechanism C to occur, the presence of at least one hydrogen on the carbon adjacent to the reactive center is required. In the absence of such a proton (for example neopentyl chlorosulfite), the mechanisms A' (ionization to give Cl<sup>-</sup> and RSO<sub>2</sub><sup>+</sup>) or B (**TS2a**) could act. In the case of ionization, a reasonable pathway involves an ion pair return, Cl<sup>-</sup> to RSO<sub>2</sub><sup>+</sup>, to the front side of the substrate through a transition structure similar to **TS2a** (the pathway through a transition structure similar to **TS3a** is not possible). As can be seen in the Table S2 (see ESI), the free energy barrier of **TS2a1** in acetonitrile is 39.5 kcal mol<sup>-1</sup>. This value is 7.9 kcal mol<sup>-1</sup> higher than **TS3a** which may explain the low reactivity of the neopentyl chlorosulfite with respect to a primary substrate such as ethyl chlorosulfite **2a**.

Another experimental data that indirectly reinforces the mechanism C suggested by us is related to the presence of the chiral chlorosulfite. Hudson et al. reported that neopentyl chlorosulfite shows an AB<sub>9</sub> system in the <sup>1</sup>H NMR spectra.<sup>29</sup> Upon raising the temperature of undiluted neopentyl chlorosulfite to 100 °C, a partial collapse of the AB pattern was observed. This is thought to be due to the onset of chlorine-chlorine exchange between molecules, each exchange being accompanied with inversion of configuration at the sulfur tetrahedron and causing loss of asymmetry for the time averaged environment of the protons of the methylene group (see **TS-II** in Scheme 4). Nevertheless, Schreiner, Schleyer and Hill<sup>16</sup> prefer to postulate that chlorine exchange is due to an ionization process rather than an inversion. This premise is used to support the S<sub>N</sub>i mechanism through an ionization process with formation of RSO<sub>2</sub><sup>+</sup> and Cl<sup>-</sup> ions (see path-I in Scheme 4). In order to computational study this chlorine exchange we carried out a study, using methyl chlorosulfite as a model, of the proposal of Schreiner, Schleyer and Hill (path-I



Scheme 4 Chlorine exchange in methyl chlorosulfite

in Scheme 4) and Hudson et al. (path-III in Scheme 4). Additionally, we also studied two new possible alternatives: Path-II where the chlorine exchange occurs through an inversion similar to that of Walden in amines and path-IV similar to Hudson's proposal but with the intervention of three methyl chlorosulfite molecules.

The results in acetonitrile indicate (see Table S3 of the ESI), that the mechanism suggested by Schreiner, Schleyer and Hill is the most unfavorable ( $\Delta G=35.6$  kcal mol<sup>-1</sup>). The Hudson mechanism is more reasonable ( $\Delta G=22.8$  kcal mol<sup>-1</sup>). But the mechanism suggested by us, through TS-III, is the most favorable from an energetic point of view ( $\Delta G=16.8$  kcal mol<sup>-1</sup>). Finally, it should be noted that, depending on the reaction conditions, other mechanisms (S<sub>N</sub>2 and E2) to convert a primary alkanesulfonyl chloride into either an olefin or the corresponding chloride can compete with the paths A-C herein studied (see Scheme S1a of the ESI for more details).

#### 2.4 Conversion of isopropyl chlorosulfite (2b) into 2-chloropropane (3b)

The relative energies ( $\Delta G$ ) in gas-phase, DCM and CH<sub>3</sub>CN associated with the conversion of **2b** into **3b** are given in Fig. 3 (see also Table S4 and Fig. S1b-1/S3b-3 of the ESI). Fig. 4 shows the geometries of the more relevant species.

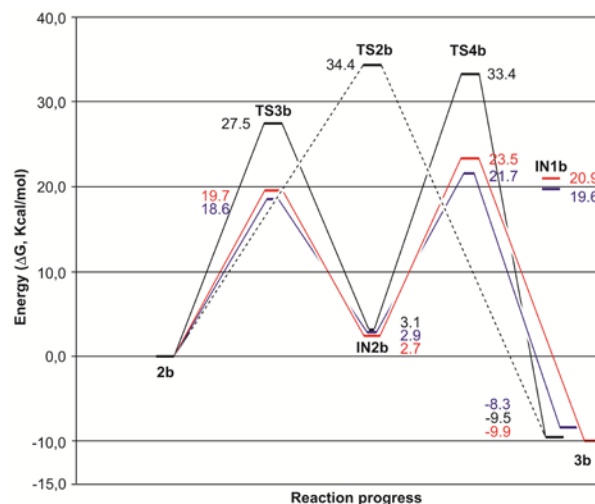


Fig. 3 Free energy profile ( $\Delta G$  in Kcal mol<sup>-1</sup>) for the conversion of **2b** into **3b** in vacuo (in black), DCM (in red) and CH<sub>3</sub>CN (in blue). The striped and solid lines correspond to the path B and path C (Scheme 2), respectively. The free energy of the ion-pair **IN1b** is also shown (in DCM and CH<sub>3</sub>CN).

#### 2.4.1 In gas-phase.

It was possible to locate **TS2b** corresponding to the path B (Scheme 2), and **TS3b**, **TS4b**, **IN2b** corresponding to the path C suggested by us.

The Gibbs free energy of the transition structure **TS4b** is 33.4 kcal mol<sup>-1</sup> higher than that of **2b** (but 1.0 kcal mol<sup>-1</sup> lower to  $\Delta G$  of **TS2b**), being in this case the rate limiting step for the conversion of **2b** into **3b**. Therefore, in terms of energy in gas-phase, the path C (Scheme 2) is more favorable than the path B (Scheme 2) (see 2.4.1-extended of the ESI for more details).

#### 2.4.2 Solvent effects in geometries, charges and energies.

The calculations in DCM and CH<sub>3</sub>CN for the species (CH<sub>3</sub>)<sub>2</sub>CHOSO<sup>+</sup> + Cl<sup>-</sup>, (CH<sub>3</sub>)<sub>2</sub>CH<sup>+</sup> + SO<sub>2</sub>Cl<sup>-</sup> indicate a higher stability of ions (CH<sub>3</sub>)<sub>2</sub>CH<sup>+</sup> + SO<sub>2</sub>Cl<sup>-</sup> (see Table S4 of the ESI) and therefore, the preference of an ionization process through path A in Scheme 2. All attempts to locate the corresponding ion pair **IN1b** starting from different initial geometries gave disappointing results. In all cases, it evolves to the final product **3b** or the intermediate **IN2b**. It was only possible to

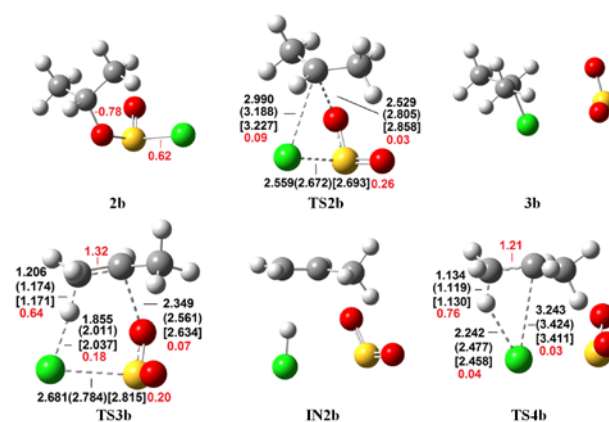


Fig. 4 Geometries, in gas-phase, of the species involved in the conversion of chlorosulfite **2b** into chloride **3b**. The bond lengths (in black) are given in angstroms. Values in parentheses and in brackets correspond to the bond lengths in DCM and CH<sub>3</sub>CN, respectively. The bond order (BO), in red.

obtain the intermediate **IN1b** with the distance C-H and the rotation of the methyl group frozen (see Fig. S4b of the ESI). The calculated energies ( $\Delta G$ ) of ion pair **IN1b** were 20.9 and 19.6 kcal mol<sup>-1</sup> in DCM and acetonitrile, respectively. This ion pair will evolve by Cl<sup>-</sup> ion attack, through a TS similar to **TS4b**, to the final product **3b** or by abstraction of a proton, through a TS similar to **TS3b**, to the intermediate **IN2b**.

On the other hand, **TS2b** could only be obtained by keeping the rotation of the methyl groups frozen, with a free energy barrier of 24.3 kcal mol<sup>-1</sup> in DCM and 22.6 kcal mol<sup>-1</sup> in CH<sub>3</sub>CN (not shown in Fig. 3). This energy barrier is higher to that obtained for the mechanism C suggested by us through **TS3b** and **TS4b** in both DCM ( $\Delta G = 19.7$  and 23.5 kcal mol<sup>-1</sup>, respectively) and CH<sub>3</sub>CN ( $\Delta G = 18.6$  and 21.7 kcal mol<sup>-1</sup>, respectively).

Again, the inclusion of the solvent does not produce significant geometric changes to the transition structures **TS2b**, **TS3b** and **TS4b** (Fig. 4). On increasing the polarity (gas-phase < DCM < CH<sub>3</sub>CN), it is observed a light increase in the length of the bonds either being formed or broken. On the other hand, the length of these bonds is greater than the corresponding distances in **TS2a**, **TS3a** and **TS4a**. The exception are the bonds H-C(2) in **TS3b** and **TS4b** in which the increase in polarity produces a shorter bond (except in **TS4b** in acetonitrile). The length of these bonds is less than the corresponding distances in **TS2a**, **TS3a** and **TS4a**. This lengthening and shortening of the bonds in **TS2b**, **TS3b** and **TS4b** with respect to **TS2a**, **TS3a** and **TS4a** is also reflected in the BO (see Fig. 2 and 4).

All the obtained transition structures were found to possess an important carbocationic character, which increases with the increase in polarity (Table S9 of the ESI). In any medium, the transition structure **TS3b** possesses the least carbocationic character while **TS4b** has the highest carbocationic character. As expected, there is an increase in the carbocationic character of **TS3b** and **TS4b** with respect to **TS3a** and **TS4a** as we move from primary substrates to secondary substrates.

The inclusion of the solvent produces a moderate stabilization of **2b**, **IN2b** and **3b** with lesser ionic character (between 3.5 and 4.7 kcal mol<sup>-1</sup>) and a strong stabilization of **TS3b** and **TS4b** (between 11.9 and 16.6 kcal mol<sup>-1</sup>) in agreement with their higher cationic character (see Table S4 of the ESI). Overall, the free energy barrier for the conversion of **2b** into **3b**, regardless of the mechanism, is lower than the free energy barrier for the conversion of **2a** into **3a**, previously studied.

Again, it is observed a flattening around the transition structures in the corresponding IRCs when passing from the gas-phase to solvents of increasing polarity (compare Fig. S2b-1/S2b-3 and S3b-1/S3b-3 of the ESI).

With independence of the medium, the transition structure **TS4b** is about 1 kcal mol<sup>-1</sup> more stable than the transition structure **TS2b**. Based on these results we can suggest that for a secondary substrate the preferred mechanism, for the conversion of an alkyl chlorosulfite into the corresponding chloride with retention of configuration, would be through the two steps (**TS3b** and **TS4b**) of path C. As in the case of the conversion of **2a** to **3a**, other mechanisms (S<sub>N</sub>2 and E2) to convert a secondary alkanesulfonyl chloride into either an

olefin or the corresponding chloride can compete with the paths A-C herein studied (see Scheme S1b of the ESI for more details).

#### 2.4.3 Effect of the solvent including explicit solvent molecules.

Due to the presence of ionic pairs, we performed a more precise study by the introduction of explicit solvent molecules. The solvent used was acetonitrile. All calculations were carried out at B3LYP/6-31G\*\* level using the SCRF-PCM method. Four molecules of acetonitrile were used for solvation. The acetonitrile molecules were positioned such that N was near positive charged centers (protons and S) and acetonitrile methyl hydrogens near the negatively charged centers (Cl and O) (see Fig. 5).

There are three distinct types of ion pairs, depending on the extent of solvation of the two ions: *fully solvated*, *solvent-shared* and *contact*. When both ions have a complete primary solvation sphere, the ion pair may be termed *fully solvated*. When there is about one solvent molecule between cation and anion, the ion pair may be termed *solvent-shared*. Lastly, when the ions are in contact with each other, the ion pair is termed a *contact* ion pair. Only *contact* and *solvent-shared* ion pairs were considered for calculation.

The results of the geometries and energies are shown in Fig. 5 (see also Table S6 of the ESI).

Species **2b-s**, **IN1b-contact-s**, **TS3b-s**, **IN2b-s** and **TS4b-s** were minimized keeping the core frozen and acetonitrile molecules aligned with the nearest proton. Only **IN1b-shared-s** was totally optimized.

The ionic pair **IN1b-shared-s** is 6.2 kcal mol<sup>-1</sup> more stable than

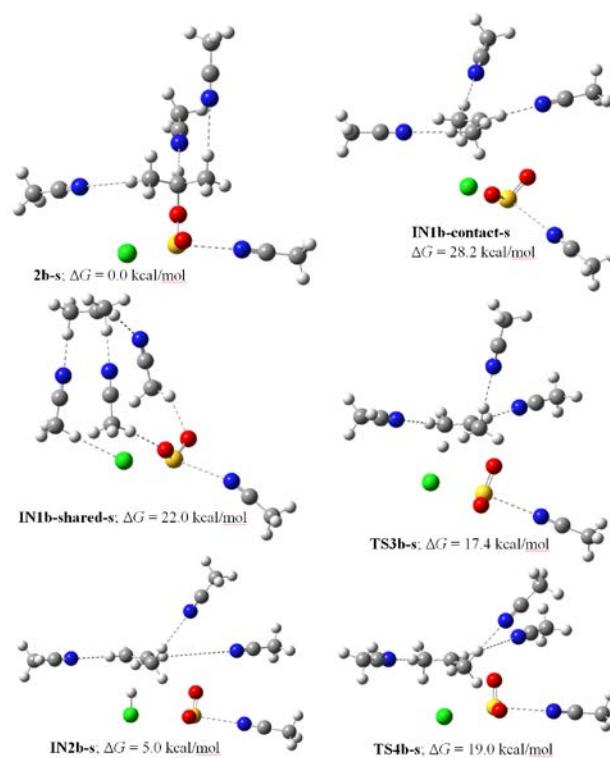


Fig. 5 Geometries in acetonitrile of the species, solvated with four molecules of acetonitrile, involved in the conversion of chlorosulfite **2b** into chloride **3b**.  $\Delta G$  relatives to **2b-s**.

**IN1b-contact-s.** Comparing the results with those obtained for the unsolvated species (Fig. 3), a slight stabilization of **TS3b-s** and **TS4b-s** is observed with free energy values of 17.4 and 19.0 kcal mol<sup>-1</sup>, respectively. The most interesting fact is that these last two values are lower than the value of 22.0 kcal mol<sup>-1</sup> obtained for the more favourable ion pair **IN1b-shared-s**. This circumstance reinforces our hypothesis of mechanism C suggested by us against mechanism A through ion pairs.

### 2.5 Conversion of *tert*-butyl chlorosulfite (**2c**) into 2-chloro-2-methylpropane (**3c**)

The relative energies ( $\Delta G$ ) in gas-phase, DCM and CH<sub>3</sub>CN associated with the conversion of **2c** into **3c** are given in Fig. 6 (see also Table S5 and Fig. S1c-1/S3c-3 of the ESI). Fig. 7 shows the geometries of the more relevant species.

#### 2.5.1 In gas-phase.

All attempts to locate **TS2c** corresponding to the path B (Scheme 2) were unsuccessful. It was only possible to locate **TS3c**, **TS4c** and intermediate **IN2c** corresponding to the path C suggested by us. **TS3c** and **TS4c** have free energy barriers of 21.8 and 22.8 kcal mol<sup>-1</sup>, respectively, appreciably lower than that found for **TS3a/TS4a** and **TS3b/TS4b**. Therefore, in terms of energy in gas-phase, the path C (Scheme 2) is the only possible one (see 2.5.1-extended of the ESI for more details).

#### 2.5.2 Solvent effects in mechanism, geometries, charges and energies.

The inclusion of the solvent in both DCM and acetonitrile produces an important change in the reaction mechanism. Firstly, it is necessary to emphasize the presence in that mechanism of the carbocation intermediate *t*-Bu<sup>+</sup> in the form of ion pair **IN1c** (*t*-Bu<sup>+</sup> + SO<sub>2</sub>Cl<sup>-</sup>). **IN1c** is stabilized by three hydrogen bonds, two O --- H and one Cl --- H (see Fig. 7). Free energy values for **IN1c** in DCM and acetonitrile are 10.8 and 9.0 kcal mol<sup>-1</sup>, respectively, above the energy value of *tert*-butyl chlorosulfite **2c**.

The intermediate **IN1c** is obtained through the transition structure **TS1c** with free energy barriers of 12.0 and 11.0 kcal

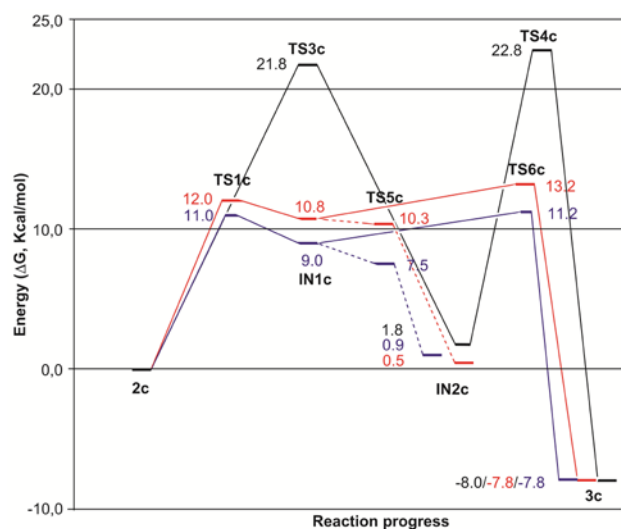


**Fig. 6** Free energy profile ( $\Delta G$  in Kcal mol<sup>-1</sup>) for the conversion of **2c** into **3c** in vacuo (in black), DCM (in red) and CH<sub>3</sub>CN (in blue). The striped lines correspond to a variation of the mechanism in DCM and CH<sub>3</sub>CN.

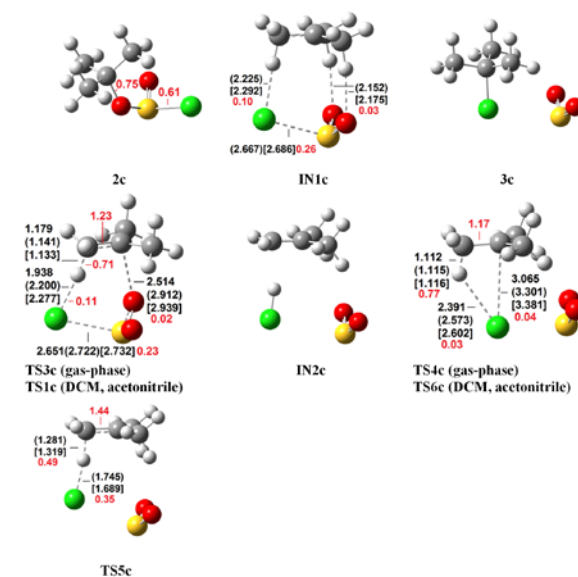


**Fig. 7** Geometries, in gas-phase, of the species involved in the conversion of chlorosulfite **2c** into chloride **3c**. The geometries of **IN1c** and **TS5c** are in dichloromethane. The bond lengths (in black) are given in angstroms. Values in parentheses and in brackets correspond to the bond lengths in DCM and CH<sub>3</sub>CN, respectively. The bond order (BO), in DCM, is in red.

mol<sup>-1</sup>, in DCM and acetonitrile, respectively.

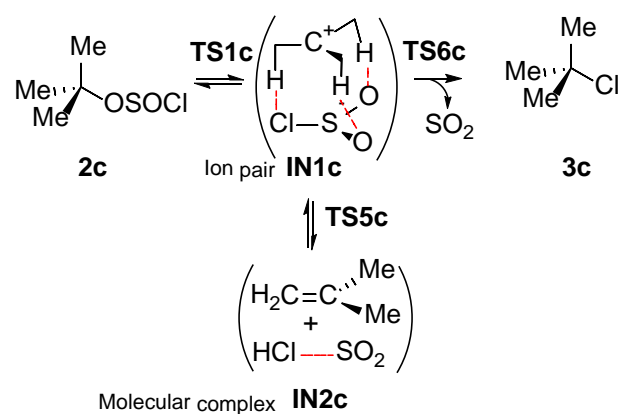
The geometry of **TS1c** is practically the same as the geometry of **TS3c** in gas-phase (see Fig. 7). However, as it has been seen in the corresponding relaxed scans (Fig. S1c-2 and S1c-3 of the ESI), the transition structure **TS1c** connects the starting product **2c** with the ion pair **IN1c** and not with the molecular complex **IN2c**.

The intermediate **IN1c** evolves through **TS5c** to the molecular complex **IN2c**. The barrier of this process is very small if we consider  $\Delta E$  (between 0.7 and 1.4 kcal mol<sup>-1</sup>) or barrierless if we consider  $\Delta G$ . The molecular complex **IN2c** is quite stable with a free Gibbs energy of 0.5 kcal mol<sup>-1</sup> (in DCM) and 0.9 kcal mol<sup>-1</sup> (in acetonitrile) higher than **2c**.

The final conversion to the chloride **3c** is carried out through **TS6c** with free energy barriers of 2.4 kcal mol<sup>-1</sup> (in DCM) and 2.2 kcal mol<sup>-1</sup> (in acetonitrile) from **IN1c**. The geometry of **TS6c** is practically the same of **TS4c** in gas-phase (see Fig. 7). However, as it can be seen in the corresponding IRCs (Fig. S2c-2 and S2c-3 of the ESI), the transition structure **TS6c** connects the final product **3c** with the ion pair **IN1c** and not with the molecular complex **IN2c**.

The overall process for the transformation of *tert*-butyl chlorosulfite **2c** into 2-chloro-2-methylpropane **3c** is outlined in Scheme 5. The path can be considered as a hybrid between path C and A of Scheme 2.

The initial chlorosulfite **2c** is transformed into the ion pair **IN1c** through **TS1c**. As a consequence of the small energy barriers involved, the ion pair **IN1c** is in equilibrium with the initial product **2c** and the molecular complex **IN2c** through **TS5c**. Finally, through **TS6c** the final product **3c** is obtained. The driving force of the whole process is the greater stability of the final product **3c** together with the expulsion of SO<sub>2</sub>.



**Scheme 5** Overall process for the conversion of **2c** into **3c**

Due to the tertiary nature of the substrate, these species present a high carbocationic character (see **2c**, **3c**, **IN2c**, **TS3c/TS1c** and **TS4c/TS6c** in Table S10). The new transition structure **TS5c** and the ion pair **IN1c** show less cationic character than **TS3c/TS1c** and **TS4c/TS6c**. This is possibly due to the dispersion of the charge produced by the hydrogen bonds present in both species.

It should be noted that the free energy barrier for the conversion of **2c** into **3c** is lower than the free energy barrier for the conversion of **2a** into **3a** and **2b** into **3b**, previously studied. This free energy barrier so low is in agreement with the difficulty for the isolation of tertiary chlorosulfites due to its rapid decomposition.<sup>16</sup> However, it has been possible to identify them by NMR spectroscopy at low temperature.<sup>30</sup> There is also a large flattening around the transition structures in the corresponding IRCs or relaxed scans (see Fig. S1c-2, S1c-3, S2c-2, S2c-3, S3c-2 and S3c-3 of the ESI).

As in the case of the conversion of **2a** to **3a** and **2b** to **3b**, other mechanisms (E1, E2, S<sub>N</sub>1) to convert a tertiary alkanesulfonyl chloride into either an olefin or the corresponding chloride can compete with the paths herein studied (see Scheme S1c of the ESI for more details).

### 2.5.3 Effect of the solvent including explicit solvent molecules.

A study similar to **2b** was performed with the explicit inclusion of four molecules of acetonitrile. The results of the geometries and energies are shown in Fig. 8 (see also Table S6 of the ESI). Species **2c-s**, **TS1c-s**, **IN2c-s**, **TS6c-s** and **TS5c-s** were minimized keeping the core frozen and acetonitrile molecules aligned with the nearest proton. **IN1c-contact-s** and **IN1c-shared-s** were totally optimized. In this case a clear difference was observed with respect to the stability of the ion pairs, being much more stable the ion pair **IN1c-contact-s** ( $\Delta G=4.5$  kcal mol<sup>-1</sup> versus 14.1 kcal mol<sup>-1</sup>). Comparing the results with those obtained for the unsolvated species (Fig. 6), is observed again a stabilization of **TS1c-s**, **TS6c-s** and **TS5c-s**, with free energy values of 8.1, 9.0 and 6.2 kcal mol<sup>-1</sup>, respectively. The energy values obtained do not substantially modify the proposed mechanism.

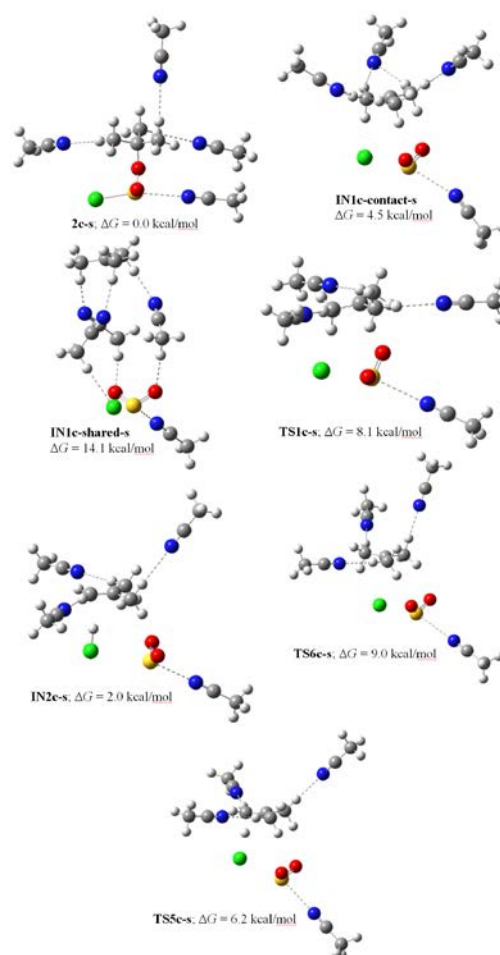


**Fig. 8** Geometries in acetonitrile of the species, solvated with four molecules of acetonitrile, involved in the conversion of chlorosulfite **2c** into chloride **3c**.  $\Delta G$  relatives to **2c-s**.

### 2.6 Effect of calculation level

In order to verify that the results obtained using the B3LYP/6-31G\*\* are correct, the main species involved in the studied mechanisms were optimized, in DCM and CH<sub>3</sub>CN, using MPWB1K/6-31++G\*\*. This level of theory has shown to have good results for combinations of thermochemistry and thermochemical kinetics in processes including weak interactions.

Also single point at B3LYP-D3/def2TZVP level and M062X/cc-pVTZ level over MPWB1K geometries (B3LYP-D3/def2TZVP//MPWB1K/6-31++G\*\* and M062X/cc-pVTZ//MPWB1K/6-31++G\*\*) were performed in acetonitrile.

The energies associated with the conversion of **2a** into **3a**, **2b** into **3b** and **2c** into **3c** are given in Table S7 of the ESI, while a schematic representation of the free energy profile at MPWB1K/6-31++G\*\* level is shown in Fig. 9.

We can summarize the observed changes, with respect to B3LYP/6-31G\*\* level, as follows:

- At MPWB1K/6-31++G\*\* level there is an increase in free energy between 1.3 and 5.9 Kcal mol<sup>-1</sup> of all transition structures and intermediate species in relation to **2** (see Fig. 9 and compare Tables S1, S4 and S5 with Table S7 of the ESI).

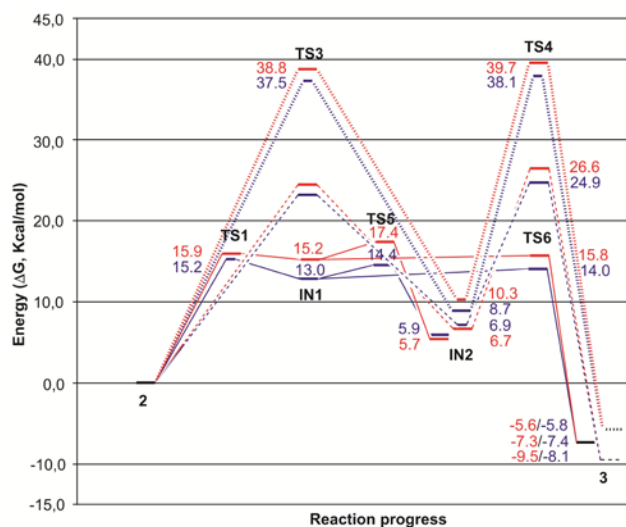


Fig. 9. Free energy profile ( $\Delta G$  in Kcal mol<sup>-1</sup>) for the conversion of **2a** into **3a** (hashed lines), **2b** into **3b** (striped lines) and **2c** into **3c** (solid lines) in DCM (in red) and CH<sub>3</sub>CN (in blue) at MPWB1K/6-31++G\*\* level.

- A similar situation is observed at M062X/cc-pVTZ level. In this case the increase in free energy is higher (between 2.5 and 8.3 Kcal mol<sup>-1</sup>; compare Tables S1, S4 and S5 with Table S7 of the ESI).

- At B3LYP-D3/def2TZVP level the situation changes and there is a decrease in free energy between 1.7 and 5.2 Kcal mol<sup>-1</sup> of all transition structures and intermediate species in relation to **2** (compare Tables S1, S4 and S5 with Table S7 of the ESI).

However, these variations do not significantly affect the reaction profile and we can therefore conclude that the results obtained at B3LYP/6-31G\*\* level can be considered adequate.

### 3. Summary and Conclusions

In summary, a study of the classic internal nucleophilic substitution mechanism S<sub>N</sub>i by means of computational studies at B3LYP/6-31G\*\*, MPWB1K/6-31++G\*\*, B3LYP-D3/def2TZVP and M062X/cc-pVTZ level in gas-phase, DCM and acetonitrile has been carried out. The study focused mainly on the comparison between the mechanisms postulated to date for the S<sub>N</sub>i mechanism (path A/A' and path B) and the new mechanism suggested by us (path C). The comparative study has been applied to the conversion of a chlorosulfite ester into an alkyl chloride. We have carried out computational studies using ethyl chlorosulfite (**2a**) (and neopentyl chlorosulfite) as a primary substrate, isopropyl chlorosulfite (**2b**) as a secondary substrate, and *tert*-butyl chlorosulfite (**2c**) as a tertiary substrate. Due to the presence of ionic pairs, we performed a more precise study, for **2b** and **2c**, by the introduction of explicit solvent molecules (acetonitrile).

In the path A/A', the chlorosulfite ester is converted, through an ionization process, into an ion pair. This ion pair undergoes front-side attack of the Cl<sup>-</sup> and loss of SO<sub>2</sub> to give the alkyl chloride with retention of configuration. The path B corresponds to the direct conversion, via a 4-center rearrangement (TS<sub>2</sub>), of the chlorosulfite ester into the alkyl

chloride. Finally, the path C occurs through two transition structures TS<sub>3</sub> and TS<sub>4</sub>. The transition structure TS<sub>3</sub> is a 6-center *syn*-rearrangement of the alkanesulfonyl chloride that produces the corresponding olefin by simultaneous expulsion of the HCl and SO<sub>2</sub>. The olefin, HCl and SO<sub>2</sub> form a molecular complex (IN<sub>2</sub>). The *syn* addition of HCl to the olefin through the transition structure TS<sub>4</sub> leads to the alkyl chloride **3** with retention of configuration.

The study led to three main conclusions:

- For a primary substrate, the mechanism suggested by us through two transition structures (path C) is more favorable than the mechanism through one transition structure (path B), both in gas phase and in solvent. Only in very polar solvents such as acetonitrile the ionization mechanism can co-occur (ionization to ROSO<sup>+</sup> and Cl<sup>-</sup>, path A').

- For a secondary substrate, the mechanism suggested by us through two transition structures (path C) is more favorable than the mechanism through one transition structure (path B) and the ionization mechanism (path A), both in gas phase and in solvent.

In acetonitrile, by the introduction of explicit solvent molecules, the ionization mechanism through a *solvent-shared* ion pair (R<sup>+</sup>--acetonitrile--SO<sub>2</sub>Cl<sup>-</sup>) is disfavoured against the mechanism C.

- For a tertiary substrate the scenario changes remarkably. In gas phase, the only reasonable mechanism is the two-stage mechanism (path C). In solvent, the most likely mechanism is a variation of the mechanism in two stages (path C) with the intervention of *contact* ionic pairs. In this case, the initial chlorosulfite is transformed into an ion pair R<sup>+</sup>SO<sub>2</sub>Cl<sup>-</sup> in equilibrium with a more stable molecular complex R'<sub>2</sub>C=CH<sub>2</sub>-HCl-SO<sub>2</sub>, which undergoes regio- and stereoselective addition of HCl.

Finally, it should be noted that depending on the reaction conditions and the nature of the substrate other mechanisms (E1, E2, S<sub>N</sub>1, S<sub>N</sub>2,) to convert an alkanesulfonyl chloride into either an olefin or the corresponding chloride can compete with the paths studied.

From an experimental point of view, our proposed mechanism explains a) the presence of olefins in this reaction type, b) the low reactivity of systems without hydrogens on the carbon adjacent to the reactive center, a key fact inexplicable by current accepted mechanisms. For the mechanism C to occur, the presence of at least one hydrogen on the carbon adjacent to the reactive center is required. In the absence of such a proton (for example neopentyl chlorosulfite), the mechanisms A/A' or B with greater energy barrier could act, thus lowering the reaction rate.

### Conflicts of interest

There are no conflicts to declare.

### Acknowledgements

This study was supported by intramural grant 201680I008 from the Spanish Government (Consejo Superior de Investigaciones Científicas).

## Notes and references

- 1 E. S. Lewis and C. E. Boozer, *J. Am. Chem. Soc.*, 1952, **74**, 308–311.
- 2 S. S. Chaudhari and K. G. Akamanchi, *Synlett*, 1999, 1763–1765.
- 3 H. R. Hudson, *Synthesis*, 1969, 112–119.
- 4 For a review of  $\text{SOCl}_2$ , see: (a) J. S. Pizey, *Synth. Reagents*, 1974, **1**, 321–357; (b) I. A. El-Sakka and N. A. Hassan, *J. Sulfur Chem.*, 2005, **26**, 33–97.
- 5 W. E. Bissinger and F. E. Kung, *J. Am. Chem. Soc.*, 1947, **69**, 2158–2163.
- 6 D. Mondal, S. Y. Li, L. Belluci, T. Laino, A. Tafi, S. Guccione and S. D. Lepore, *J. Org. Chem.*, 2013, **78**, 2118–2127.
- 7 D. J. Cram, *J. Am. Chem. Soc.*, 1953, **75**, 332–338.
- 8 C. E. Boozer and E. S. Lewis, *J. Am. Chem. Soc.*, 1953, **75**, 3182–3186.
- 9 A. Jr. Streitwieser and W. D. Schaeffer, *J. Am. Chem. Soc.*, 1957, **79**, 379–381.
- 10 D. J. Cash and P. Jr. Wilder, *Chem. Commun.*, 1966, **19**, 662–664.
- 11 J. K. Stille and F. M. Sonnenberg, *J. Am. Chem. Soc.*, 1966, **88**, 4915–4921.
- 12 H. R. Hudson and G. R. De Spinoza, *J. Chem. Soc. Perkin 1*, 1976, 104–108.
- 13 For a short review concerning  $\text{S}_{\text{N}}\text{i}$  fragmentations of alkyl chlorosulfites see: R. A. Moss, X. Fu and R. R. Sauers, *J. Phys. Org. Chem.*, 2007, **20**, 1–10.
- 14 M. A. González, J. Mancebo-Aracil, V. Tangarife-Castaño, L. Agudelo-Gómez, B. Zapata, A. Mesa-Arango and L. Betancur-Galvis, *Eur. J. Med. Chem.*, 2010, **45**, 4403–4408.
- 15 J. F. King, J. Y. L. Lam and V. Dave, *J. Org. Chem.*, 1995, **60**, 2831–2834.
- 16 P. R. Schreiner, P. von R. Schleyer and R. K. Hill, *J. Org. Chem.*, 1993, **58**, 2822–2829.
- 17 P. R. Schreiner, P. von R. Schleyer and R. K. Hill, *J. Org. Chem.*, 1994, **59**, 1849–1854.
- 18 D. Y. Curtin, and D. B. Kellom, *J. Am. Chem. Soc.*, 1953, **75**, 6011–6018.
- 19 M. J. Frisch, et al., *Gaussian 09, Revision A.02*, Gaussian, Inc., Wallingford, CT, 2009.
- 20 (a) R. G. Parr and W. Yang, *Density Functional Theory of Atoms and Molecules*, Oxford University Press, New York, 1989; (b) T. Ziegler, *Chem. Rev.*, 1991, **91**, 651–667.
- 21 (a) A. D. Becke, *J. Chem. Phys.*, 1993, **98**, 5648–5652; (b) C. Lee, W. Yang and R. G. Parr, *Phys. Rev. B*, 1988, **37**, 785–789.
- 22 W. J. Hehre, L. Radom, P. von R. Schleyer and J. A. Pople, *Ab initio Molecular Orbital Theory*, Wiley, New York, 1986.
- 23 (a) J. Tomasi and M. Persico, *Chem. Rev.*, 1994, **94**, 2027–2094; (b) B. Y. Simkin, I. Sheikhet, *Quantum Chemical and Statistical Theory of Solutions-A Computational Approach*, Ellis Horwood, London, 1995.
- 24 (a) E. Cancès, B. Mennunci and J. Tomasi, *J. Chem. Phys.*, 1997, **107**, 3032–3041; (b) M. Cossi, V. Barone, R. Cammi and J. Tomasi, *Chem. Phys. Lett.* 1996, **255**, 327–335; (c) V. Barone, M. Cossi and J. Tomasi, *J. Comp. Chem.*, 1998, **19**, 404–417.
- 25 K. Fukui, *J. Phys. Chem.*, 1970, **74**, 4161–4163.
- 26 (a) C. González and H. B. Schlegel, *J. Phys. Chem.*, 1990, **94**, 5523–5527; (b) C. González and H. B. Schlegel, *J. Chem. Phys.* 1991, **95**, 5853–5860.
- 27 (a) A. E. Reed, R. B. Weinstock and F. Weinhold, *J. Chem. Phys.*, 1985, **83**, 735–746; (b) A. E. Reed, L. A. Curtiss and F. Weinhold, *Chem. Rev.*, 1988, **88**, 899–926.
- 28 Y. Zhao and D. G. Truhlar, *J. Phys. Chem. A*, 2004, **108**, 6908–6918.
- 29 H. R. Hudson, R. G. Rees and G. R. De Spinoza, *Spectrochim. Acta*, 1971, **27(A)**, 926–929.
- 30 J. A. Hartsel, D. T. Craft, Q.-H. Chen, M. Ma and P. R. Carlier, *J. Org. Chem.*, 2012, **77**, 3127–3133.